Pergamon

Int. Comm. Heat Mass Transfer, Vol. 25, No. 8, pp. 1159–1168, 1998

0735-1933/98 $19.00 + .00

PII S0735-1933(98)00106-7

EFFECT OF ANISOTROPY ON THE DEVELOPMENT OF CONVECTIVE BOUNDARY LAYER FLOW IN POROUS MEDIA

G. Degan[1], H. Beji[2], P. Vasseur[1] and L. Robillard[1]
[1] Ecole Polytechnique, Montreal, P.Q., H3C 3A7, Canada
[2] Université de Gergy-Pontoise, 95031, France

(Communicated by J.P. Hartnett and W.J. Minkowycz)

ABSTRACT

The effects of anisotropy on the development of thermal boundary layer flow in a rectangular porous cavity is studied. The side walls of the cavity are respectively heated and cooled isothermally. Top and bottom walls are insulated. The porous medium is anisotropic both in permeability and thermal conductivity with its principal axes oriented in a direction that is oblique to the gravity vector. Scale analysis is applied to predict the orders of magnitude involved in the boundary layer regime. In the large Rayleigh number limit, the governing boundary layer equations are solved in closed form, using an integral approach. A finite difference method is used to obtain numerical solutions of the full governing equations. The effects of the anisotropy in permeability and thermal conductivity on the development of free convective boundary layer flow are found to be significant.

Introduction

Earlier studies on natural convection in a saturated anisotropic porous medium are concerned mostly with the case of a horizontal layer heated from below (Castinel and Combarnous [1], Kvernold and Tyvand [2] and Tyvand and Storesletten [3]), this configuration being of interest in some geophysical problems. These studies were mainly concerned on the effects of anisotropy in permeability on the critical Rayleigh number for the onset of convection and the behavior of convective flows at slightly supercritical Rayleigh numbers. A few studies have also been reported on natural convection in vertical enclosures containing hydrodynamically anisotropic porous media (Kimura et al. [4] and Ni and Beckermann [5]). In these investigations, the principal axes of the anisotropic medium were assumed to be coincident with the gravity vector. The permability ratio was found to cause channeling of the flow and influence considerably the flow field and the heat transfer within the cavity. The case of a porous medium, with an anisotropic permeability of arbitrary orientation, has been investigated by Degan et al. [6,7]. It was demonstrated that the heat transfer was maximum when the principal axis with higher permeability is parallel to the vertical direction, and minimum when it is perpendicular to the vertical direction. Recently, Aboubi et al. [8] have considered the anisotropic effects of the porous medium on natural convection within a horizontal annulus heated isothermally. The analogous problem of free convection in porous media with anisotropy in the thermal properties has also been studied and reported in the literature by Kimura et al. [4], Ni and Beckermann [5] and Degan and Vasseur [6]. It was demonstrated by these authors that the effect of the thermal conductivity ratio on the overall heat transfer was significant.

The objective of this study is to examine the effect of anisotropy, in permeability and thermal diffusivity, on the development of convective boundary layer flow in a rectangular porous cavity. Both a numerical approach and an analytical solution, valid in the boundary layer regime, are used to investigate the problem.

Mathematical Formulation

Figure 1 illustrates a rectangular fluid-saturated porous cavity, the coordinates system, and the thermal boundary conditions. The porous medium is assumed to be anisotropic both in permeability and thermal conductivity. The permeabilities along the two principal axes of the porous matrix are denoted by K_1 and K_2. The anisotropy in flow permeability of the porous medium is then characterized by the permeability ratio $K^* = K_1/K_2$, and the orientation angle θ, defined as the angle between the horizontal direction and the principal axis with permeability K_2. The principal directions of the thermal conductivities (k_1, k_2) are assumed to coincide with those of the permeability axes. The two vertical walls are respectively heated and cooled at temperatures T'_h and T'_c, the horizontal walls are supposed adiabatic. Generalized Darcy's law (Bear [9]) and the Boussinesq approximation are used.

Then the equations that account for the conservation of mass, momentum, and energy are as follows

$$\nabla . \overrightarrow{V'} = 0 \tag{1}$$

$$\overrightarrow{V'} = -\frac{\overline{\overline{K}}\,'}{\mu}\left[\nabla p' + \varrho \overrightarrow{g} \beta (T' - T'_r)\right] \tag{2}$$

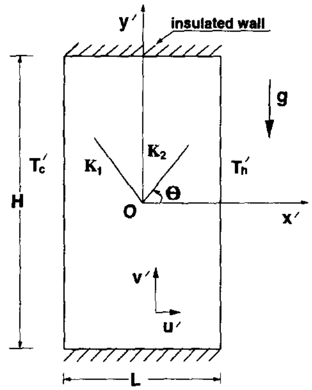

FIG. 1
The physical situation and coordinate system.

$$\frac{1}{(\varrho c)_f}\nabla.\left(\overline{\overline{k}}' \;\nabla T'\right) = \nabla.\;\left(\overrightarrow{V'}T'\right) \tag{3}$$

where $\overrightarrow{V'}$ is the superficial flow velocity, p' pressure, T' temperature, μ dynamic viscosity, ρ density, β coefficient of thermal expansion, $\vec{g}$ gravitational acceleration, $(\varrho c)_f$ heat capacity of the fluid and $\overline{\overline{K}}\,'$ and $\overline{\overline{k}}\,'$ second order permeability and thermal conductivity tensors, respectively. Subscript r indicates a reference state.

Eliminating the pressure in the momentum equation in the usual way, and taking L, α/L^2 and $\Delta T' = T_h' - T_c'$ as respective dimensional scales for length, velocity and temperature, the governing equations may be written in nondimensional form as

$$a\,\frac{\partial^2\psi}{\partial x^2} + b\,\frac{\partial^2\psi}{\partial x\partial y} + c\,\frac{\partial^2\psi}{\partial y^2} = -R\frac{\partial T}{\partial x} \tag{4}$$

$$d\,\frac{\partial^2 T}{\partial x^2} + e\,\frac{\partial^2 T}{\partial x\partial y} + f\,\frac{\partial^2 T}{\partial y^2} = u\frac{\partial T}{\partial x} + v\frac{\partial T}{\partial y} \tag{5}$$

where

$$\left.\begin{array}{ll} a = \cos^2\theta + K^*\sin^2\theta & d = \cos^2\theta + k^*\sin^2\theta \\ b = (K^* - 1)\sin 2\theta & e = (1 - k^*)\sin 2\theta \\ c = \sin^2\theta + K^*\cos^2\theta & f = \sin^2\theta + k^*\cos^2\theta \end{array}\right\} \tag{6}$$

and ψ is the dimensionless stream function defined as $u = \partial\psi/\partial y$ and $v = -\partial\psi/\partial x$ such that the continuity equation (1) is automatically satisfied.

The non-dimensional boundary conditions over the walls of the enclosure are

$$x = 1/2: \qquad \psi = 0 \qquad T = 1 \tag{7}$$

$$x = -1/2: \qquad \psi = 0 \qquad T = 0 \tag{8}$$

$$y = \pm A/2: \qquad \psi = 0 \qquad \frac{\partial T}{\partial x} = 0 \tag{9}$$

where $A = H/L$ is the cavity aspect ratio, $k^* = k_1/k_2$ the thermal diffusivity ratio and R is the Rayleigh number $R = K_1 g\beta\Delta T' L/(\alpha\nu)$ based on the permeability K_1, and the thermal diffusivity $\alpha = k_2/(\varrho c)_f$.

The overall heat transfer rate across the enclosure is expressed by the average Nusselt number at the right vertical wall, defined as

$$Nu = -\frac{1}{A}\int_0^A \left.\frac{\partial T}{\partial x}\right|_{x=1/2} dy \tag{10}$$

From the above governing equations and boundary conditions it is seen that the present problem is governed by five dimensionless parameters: the Rayleigh number R , the aspect ratio of the cavity A, the flow permeability ratio K^*, the thermal conductivity ratio k^* and the angle of the principal axes θ.

Numerical solution

Numerical solutions of the governing equations are obtained using a standard finite difference numerical method. A successive overrelaxation method, is used to solve equation (4). The energy equation (5), in its time dependant form, is solved by an alternating direction implicit method. All derivatives are discretized according to the Taylor-based second order central difference scheme. Integration in time was continued until a convergence criterion of 0.1% was satisfied. The difference between the global Nusselt number at hot and cold walls was within 0.1%. The rectangular domain was divided into a uniform mesh. Convergence with mesh size was verified by employing coarser and finer grids on selected test problems. Based on these results a mesh size 80×50 was adopted for most of the cases considered in this study.

Boundary Layer Analysis

In the boundary layer regime, most of the buoyancy-induced flow circulation is restricted to a thin layer $\delta = \delta'/H << 1$) along each verticall wall. For this situation, it is readily demonstrated that the conservation statements (4) and (5) yield the following boundary layer scales

$$\left.\begin{array}{rcl} \delta & \sim & A^{1/2}\, d^{1/2}\, a^{1/2}\, R^{-1/2} \\ \psi & \sim & A^{1/2}\, d^{1/2}\, a^{-1/2}\, R^{1/2} \\ u & \sim & A^{-1/2}\, d^{1/2}\, a^{-1/2}\, R^{1/2} \\ v & \sim & a^{-1}\, R \end{array}\right\} \tag{11}$$

The average Nusselt number, defined as the total heat transfer rate from one side wall to the other q', over the heat transfer rate in the pure heat conduction limit q_c', has the following scale

$$Nu = \frac{q'}{q_c'} = \frac{k_2 H \Delta T'/\delta'}{k_2 H \Delta T'/L} \sim A^{-1/2}\, d^{-1/2}\, a^{-1/2}\, R^{1/2} \tag{12}$$

The boundary layer scales, Eq. (11), suggest the following nondimensionalization of the governing equations (4) and (5) in the boundary layer region

$$\frac{\partial^2 \overline{\psi}}{\partial \overline{x}^2} = - \frac{\partial \overline{T}}{\partial \overline{x}} \tag{13}$$

$$\overline{u}\frac{\partial \overline{T}}{\partial \overline{x}} + \overline{v}\frac{\partial \overline{T}}{\partial \overline{y}} = \frac{\partial^2 \overline{T}}{\partial \overline{x}^2} \tag{14}$$

when the following variables are used

$$\left.\begin{array}{ccc} \overline{x} = \dfrac{x\, L}{\Lambda} & \overline{y} = \dfrac{y}{A} & \overline{\psi} = \psi\dfrac{\Lambda}{H\, d} \\ \overline{u} = u\,\dfrac{\Lambda}{d\, L} & \overline{v} = v & \overline{T} = T \\ & \Lambda^2 = \dfrac{L\, H\, a\, d}{R} & \end{array}\right\} \tag{15}$$

Using the same notation, the boundary conditions, for the boundary layer lining the left wall in Fig. 1, are $\overline{\psi} = 0$ and $\overline{T} = 0$ on the the wall and $\overline{\psi} = \overline{\psi}_\infty(\overline{y})$ and $\overline{T} = \overline{T}_\infty(\overline{y})$ in the core where $\overline{\psi}_\infty(\overline{y})$ and $\overline{T}_\infty(\overline{y})$ are unknown and represent the velocity and temperature distributions in the core of the cavity, sufficiently far from the boundary layer region.

The dimensionless nonlinear governing equations (13) and (14), together with boundary conditions are exactly the same as those considered by Simpkins and Blythe [10] while studying boundary layer flows within an isotropic porous cavity. Translating their results for their two-layers profile model into the present notation, it is readily found that, the value of the stream function at the center of the cavity ($x = 0$, $y = 0$) is given by

$$\psi_C = 0.734 \left(A \frac{dR}{a}\right)^{1/2} \tag{16}$$

The overall heat transfer rate between the two side walls is given by

$$Nu = 0.51 \left(\frac{R}{A\, a\, d}\right)^{1/2} \tag{17}$$

The agreement between the above results and the order of magnitude prediction, Eqs. (11) and (12), is evident.

Results and Discussion

Past studies concerning the effects of anisotropic permeability on natural convection have focussed mostly on the boundary layer regime ($R \to \infty$). Intuitively, it is expected that unidirectional flows, including boundary layer type, must somehow depend on the characteristics of the anisotropic porous medium in the flow direction. This point is confirmed by the analytical results obtained here under the boundary layer approximations. For this situation it is found for instance that, according to Eq. (17), the Nusselt number for a porous medium with isotropic thermal conductivity ($k^* = 1$, i.e. $d = 1$) is given by $Nu = 0.51(R/(A\ a))^{1/2}$. This results clearly indicates that, for boundary layer flows, the appropriate Rayleigh number is $\overline{R} = R/a = g\beta\Delta T' L/(\alpha\nu P_{yy})$ where $P_{yy} = a/K_1$ is the y-component of the hydraulic resistivity tensor $\overline{\overline{P}} = [\overline{\overline{K}}]^{-1}$. In terms of this directional hydraulic resistivity the problem is considerably simplified since the porous medium can then be treated as an isotropic one.

The effects of anisotropy in flow permeability on natural convection at low Rayleigh numbers will be now discussed. When the convective motion is small enough, such that the boundary layer approximations cannot be invoked, the problem depends then on the full hydraulic resistivity tensor $\overline{\overline{P}}$, defined as

$$\overline{\overline{P}} = \frac{1}{K_1} \begin{bmatrix} c & b/2 \\ b/2 & a \end{bmatrix} \tag{18}$$

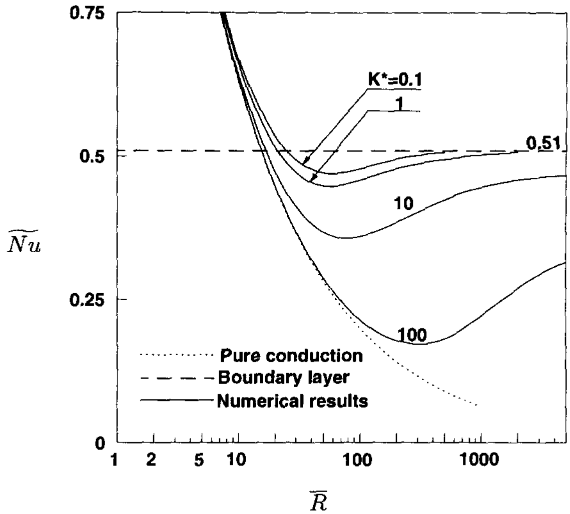

FIG. 2
Effects of $\overline{R}$ and K^* on $\widetilde{Nu}$ for $A = 4$, $\theta = 0^o$ and $k^* = 1$.

For this situation, in view of the complex nature of the problem, a numerical solution appears to be the only approach. The numerical results presented in Figs. 2 and 3 illustrate the effects of the modified Rayleigh number $\overline{R} = R/a$, the permeability ratio K^* and the anisotropy orientation angle θ on the modified Nusselt number $\widetilde{Nu} = Nu(A/\overline{R})^{1/2}$. The range of the governing parameters considered here covers the gap between the pure conductive regime $\widetilde{Nu} = (A/\overline{R})^{1/2}$, and the boundary layer regime, $\widetilde{Nu} = 0.51$. These two limits are depicted as dashed lines and dotted ones, respectively. From the results presented in these graphs it is clear that, for intermediate values of $\overline{R}$ between the pure conduction and the boundary layer regime, the convective heat transfer within the anisotropic porous medium, is governed by the full equation (4). For this situation the three parameters a, b, and c, characterizing the anisotropic permeability of the porous medium, are significant.

Figure 2 shows the numerical results obtained for $A = 4$, $\theta = 0^o$, k^* and various values of K^* ($a = 1$, $b = 0$ and $c = K^*$). It is observed that, for a given value of $\overline{R}$, the value of $\widetilde{Nu}$ decreases as K^* is made larger than unity. This follows from the fact that an increase in K^* corresponds to a decrease in the permeability K_2 when other parameters are held contant ($\overline{R}$ i.e., K_1). As a result the convective motion inside the cavity is inhibited, resulting in a weaker heat transfer. Naturally, the reverse trend occurs when K^* is made smaller than unity. Also, Fig. 2 indicates that, as expected, for a given value of K^* the corresponding curve tends asymptotically towards the pure conduction regime as $\overline{R}$ is made small enough. The value of $\overline{R}$ necessary to reach this regime depends strongly upon K^*. For instance, for $K^* = 10^2$ pure conduction is reached where $\overline{R} \simeq 50$ while for $K^* = 10^{-1}$ the corresponding value is approximately $\overline{R} \simeq 5$. On the hand, when the convective motion inside the cavity is strong enough the resulting heat transfer tends asymptotically towards the boundary layer limit $\widetilde{Nu} = 0.51$, provided that $\overline{R}$ is made large enough. The Rayleigh number necessary to reach this regime is seen to increase considerably as the value of K^* is made larger.

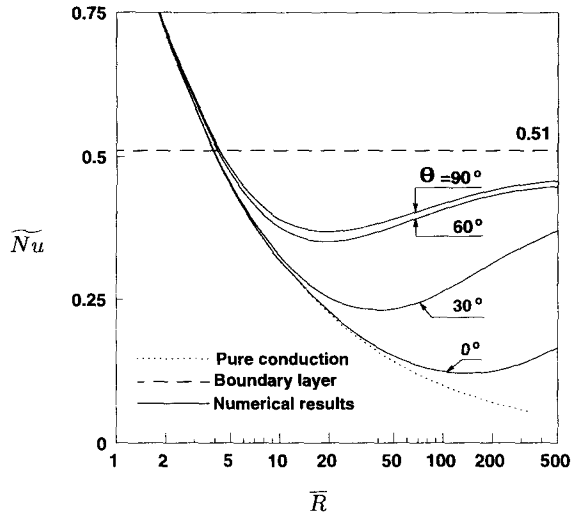

FIG. 3
Effects of $\overline{R}$ and θ on $\widetilde{Nu}$ for $A = 1$, $K^* = 10$ and $k^* = 1$.

The effects of the anisotropy orientation angle θ is illustrated in Fig. 3 for $A = 1$, k^* and $K^* = 10$. For a given value of the modified Rayleigh number $\overline{R}$ it is seen that $\widetilde{Nu}$ is minimum when $\theta = 0^o$ and maximum when $\theta = 90^o$. This follows from the fact that $a = 1$ in the first case and $a = K^* = 10$ in the second one, such that the Rayleigh number $R = \overline{R}\ a$ is ten times higher for $\theta = 90^o$ than for $\theta = 0^o$. A comparison of the results obtained for $K^* = 10$ and $\theta = 0^o$ in Figs. 2 and 3 indicates that convection is more important in the first case ($A = 4$) than in the second one ($A = 1$). For this reason the value of $\overline{R}$ necessary to reach the boundary layer regime will be considerably higher for $A = 1$ than that for $A = 4$.

When the porous matrix has an anisotropic property in both permeability and thermal conductivity the heat transfer, in the boundary layer regime, is predicted by Eq. (17). Figure 4 shows Nu versus the modified Rayleigh number $\widetilde{R} = R/(ad)$. The boundary layer solution derived in the present study is depicted on the graph as a solid line. The numerical results obtained for various values of K^*, k^* and θ are seen to be in good agreement with the analytical solution provided that $\widetilde{R}$ is made large enough. The start of the boundary layer regime is strongly dependent on the values of the anisotropic parameters.

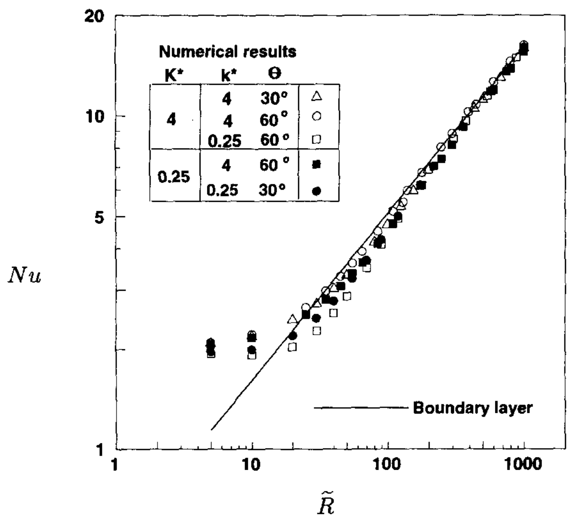

FIG. 4
Effect of $\widetilde{R}$ on Nu for $A = 4$, and various values of K^*, k^* and θ.

Acknowledgement

This work was supported in part by the Natural Sciences and Engineering Research Council, Canada and jointly by the FCAR, Government of Quebec.

Nomenclature

K_1, K_2	flow permeability along the principal axes
K^*	permeability ratio, K_1/K_2
k_1, k_2	thermal conductivity along the principal axes
k^*	thermal conductivity ratio, k_1/k_2
Nu	overall Nusselt number, Eq. (10)
$\widetilde{Nu}$	modified Nusselt number, $Nu(A/\overline{R})^{1/2}$
R	Rayleigh number, $K_1 g\beta L\Delta T'/\alpha\nu$
$\overline{R}$	Rayleigh number based on directional permeability, R/a
$\tilde{R}$	modified Rayleigh number, $R/(ad)$

Greek Symbols

α	thermal diffusivity, $k_2/(\varrho c)_f$
β	coefficient of thermal expansion of the fluid
θ	inclination of the principal axes
ν	kinematic viscosity of the fluid

References

1. G. Castinel and M. Combarnous, *C. R. Hebd. Seanc. Acad. Sci. Paris B*, 701-704 (1974).

2. O. Kvernvold and P. A. Tyvand, *J. Fluid Mech.*, 90, 609-624 (1979).

3. P. A. Tyvand and L. Storesletten, *J. Fluid Mech.*, 226, 371-382 (1991).

4. S. Kimura, Y. Masuda and T. K. Hayashi, *Heat Transfer Jap. Res.*, 22, 139-153 (1993).

5. J. Ni and C. Beckermann, *J. Heat Transfer*, 113, 1033-1037 (1991).

6. G. Degan, P. Vasseur and E. Bilgen, *Int. J. Heat Mass Transfer*, 38, 1975-1987 (1995).

7. G. Degan and P. Vasseur, *Numerical Heat Transfer*, 38, 397-412 (1996).

8. K. Aboubi, L. Robillard and E. Bilgen, Natural Convection in Horizontal Annulus Filled with an anisotropic porous medium, *ASME/JSME Thermal Engineering Conf.*, 3, 415-422 (1995).

9. J. Bear, *Dynamics of Fluid in Porous media*, Elsevier, New-York (1972).

10. P. G. Simpkins and P. A. Blythe, *Int. J. Heat Mass Transfer*, 23. 881-887 (1980).

Received April 30, 1998